A99-16503

AIAA 99-0637

Detection of the Loss of Elevator Effectiveness Due to Aircraft Icing

R. Miller and W. Ribbens
The University of Michigan
Ann Arbor, MI

37th AIAA Aerospace Sciences Meeting and Exhibit
January 11-14, 1999 / Reno, NV

AIAA-99-0637

DETECTION OF THE LOSS OF ELEVATOR EFFECTIVENESS DUE TO AIRCRAFT ICING

Robert H. Miller *
William B. Ribbens,
Department of Aerospace Engineering,
The University of Michigan, Ann Arbor, MI 48109 †

Abstract

Aircraft icing causes performance degradation in aircraft. When a significant amount of degradation occurs aircraft accidents occur which result in the lost of life and property. Currently sensors measure the amount of ice buildup only at specific points on the aircraft. Icing flight tests conducted by NASA Lewis Research Center to investigate the efects of tailplane icing. Analysis of this data indicates that it is possible to detect the onset of aircraft icing by utilizing a gain scheduled Beard-Jones Detection Filter(BJDF). Specifically the case of a failed de-icing boot is analyzed and a detection filter is formulated to detect this failure.

Introduction

This paper presents preliminary results of a technique for detecting icing by continuously estimating control surface effectiveness. That is to say the present method is less concerned with attempting to measure actual ice accretion than it is with the deleterious effects on aircraft controllability. The feasibility of the method is validated with flight test data provided by the NASA Lewis Research Center.

A study by the United Kingdom's Civil Aviation Authority indicated that all the manufacturers of aircraft and a sizeable portion of commercial pilots interviewed for the study "regarded ice detectors as unreliable" [1]. The main reason for this view is that the detectors gave spurious readings and/or late indications of icing. The majority of commercial pilots seem to believe that ice accretion is readily observable from the cockpit and that the important issue is the effectiveness of the anti-icing equipment.

There are certain circumstances where this widely held pilot opinion may be incorrect. For example tail icing is generally not observable from the cockpit. Moreover, even if the wing de-icing is successful tail de-icing might not take place, particularly in the case of a failed de-icing boot on the horizontal or vertical stabilizer.

It is the goal of the current study to detect icing by detecting the resulting changes in aircraft dynamics. The major focus for the present paper is to detect the loss of control surface effectiveness that results from icing via estimating changes in the aircraft dynamic model. In particular we consider the example of the loss of elevator effectiveness resulting from a failed de-icing boot during flight in icing conditions(although the method is generally applicable to any control surface).

Ice accumulation on the horizontal stabilizer is a potentially hazardous condition particularly during approach and landing. Among other effects icing results in a major reduction of $C_{L_{max}}$ for any iced aerodynamic surface be it the horizontal stabilizer, vertical stabilizer, or main wing. During approach and especially during final approach phase of flight the flaps are deflected, causing an increase in downwash(relative to cruise for example) that can seriously reduce the tailplane stall margin.

The concept here is to detect the loss of elevator effectiveness due to a failed de-icing boot at an early phase such that appropriate pilot action can be taken to safely complete the flight. In this method, the aircraft dynamics are continuously monitored by appropriate computer manipulation of data from the attitude and/or navigation sensors. Then once the loss of control effectiveness resulting from uncontrolled icing has been detected the flight crew can be notified through relevant display.

Other previous work, [2], has attempted to detect icing via online parameter estimation how-

*Supported in part by NASA under grant NGT4-52404

ever the present method is based upon continuously monitoring aircraft dynamics via a state estimator. This approach is highly computational efficient relative to online parameter estimation. This estimator is of the form of a gain scheduled Beard-Jones Detection Filter(BJDF), [3] and [4], which incorporates a state variable model for the aircraft dynamics in the aircraft body axes. The eigenstructure for the state estimator is chosen such that the output error residuals resulting from a hypothesized failure(eg. a failed de-icing boot on a horizontal stabilizer) are one dimensional. The hypothesized failure is readily detected by a statistically significant error residual and it can be isolated from other classes of failure by its direction in output space. Any other failure having a collinear output error residual, that is said to be detection equivalent to the hypothesized failure, produces the same change in aircraft dynamics as the hypothesized failure.

The observer/state estimator applicable for the present method is derived from a state variable model for the aircraft dynamics. This model includes the effect of icing in the input matrix, refer to the related paper, [5], for more details. Typically in practice the nonlinearity in aircraft dynamics model is handled via gain scheduling the state transition matrix as a function of operating conditions.

Normally, the robustness of such a linear model is not a major issue for the BJDF type observer since the closed loop error dynamics are designed to be at least asymptotically stable via the eigenstructure assignment. This stability is achieved during the design of the filter.

Considering the example of the failed horizontal stabilizer boot, the effect of icing that can occur on this surface include a gradual trim change as the ice accretes on the surface. In addition icing results in a dramatic change on the horizontal tail lift characteristics including a large reduction in $C_{L_{max}}$. This latter effect is manifest in the dynamic model as a change in the input matrix. This latter change is in the form of a failure event vector that is the input vector for the dynamics of the BJDF. That is, this hypothesized failure results in an error residual along a unique direction in output space associated with horizontal stabilizer icing.

In this case, detection of horizontal stabilizer icing resulting for example from a failed de-icing boot can be achieved by monitoring the output error residuals along the direction associated with that hypothesized failure. Optimal signal detection methods are potentially applicable to reduce the 2 types of detection errors.

This paper develops the models associated with such a failure and explains the design of a relevant BJDF. In addition the performance of the BJDF is demonstrated in simulation and with actual data from NASA Lewis Icing Research Aircraft, [6] flying with simulated horizontal stabilizer ice.

Aircraft Model

The detailed results of the analysis of the NASA Lewis icing research flight tests can be found in [5], [7], and [8]. The following equations, [9], were used to model the longitudinal dynamics of the twin otter icing research aircraft.

$$\begin{aligned} \dot{X} &= f(X,V) \\ \begin{bmatrix} \dot{u} \\ \dot{w} \\ \dot{\theta} \\ \dot{q} \end{bmatrix} &= \begin{bmatrix} -wq + \frac{F_x}{m} - g_x \\ uq + \frac{F_z}{m} + g_z \\ q \\ \bar{q}ScC_m/I_y \end{bmatrix} \end{aligned} \tag{1}$$

$$\begin{aligned} \bar{q} &= \frac{1}{2}\rho(u^2+w^2) & \alpha &= \tan^{-1}\left(\frac{w}{u}\right) \\ F_x &= \bar{q}SC_x + T_x, & F_z &= \bar{q}SC_z + T_z \\ g_x &= \sin(\theta)g, & g_z &= \cos(\theta)g. \end{aligned}$$

where C_x,C_z, and C_m are polynomials functions of α, q, and δ_e. A more detailed explanation of the variables and the model can be found in [5]. The functions used for the detection filter are of the form,

$$C_x = x_1\alpha + x_2\alpha^2 + x_3\delta_e + x_4 \tag{2}$$

$$C_z = z_1\alpha + z_2 q + z_3\alpha^2 + z_4\delta_e + z_5 \tag{3}$$

$$C_m = m_1\alpha + m_2 q + m_3\alpha^2 + m_4\delta_e + m_5. \tag{4}$$

The values for the different coefficients can be found in [5]. The outputs are

$$\begin{aligned} Y &= h(X) \\ Y &= \begin{bmatrix} \alpha \\ \theta \\ q \end{bmatrix} \end{aligned} \tag{5}$$

Detection Filter

The major goal of this paper is to demonstrate that the onset of tail icing in an aircraft can be modeled as a partial actuator failure and a Beard-Jones Detection Filter(BJDF), [3] and [4], can be designed to detect this failure. A BJDF is a suboptimal state estimator that is designed to constrain the error

residual due to a specific failure to a single direction in output space. In this way if one computes a statistically significant error residual in the BJDF constrained failure direction one knows a failure has taken place.

The state estimator that is implemented in a BJDF is of the form of a gain scheduled Luenberger observer which continuously computes an estimate of $\hat{x}$ of the state vector. Its dynamics are given by:

$$\dot{\hat{x}} = \bar{A}\hat{x} + \bar{B}u + D_g(y - \hat{y}) \tag{6}$$

where $\hat{y} = C\hat{x}$, and where $\bar{A}$ and $\bar{B}$ are the state transition and input matrices of the nominal reference model for the aircraft dynamics. The state vector error dynamics are of the form

$$\dot{\epsilon} = (\bar{A} - D_g C)\epsilon + f_d \tag{7}$$

where $\epsilon = x - \hat{x}$ is the state error residual and f_d is the input "failure" due to icing. Under relatively benign conditions there is sufficient design freedom(in choosing D_g) to permit the output error residuals($e = C\epsilon$) to be constrained to a one dimensional subspace. In addition, the eigenvalues can be placed as a compromise between rapid response and minimal random error due to process or measurement noise, further research is being conducted in this area.. In the above formulation the failure event vector f_d corresponds to the change in the input due to loss of control surface effectiveness.

Failure Signature

There are four separate cases, $\delta_{flap} = 0°, 10°, 20°$, and $30°$, that need to be modeled. Utilizing the models obtained in [5] a failure signature vector was developed by linearizing the nonlinear models about the current operating point and subtracting the input matrices. As expected the difference between the eigenvalues of the state transition matrices for the iced and un-iced cases was found to be negligible. Thus no changes in the A matrices needed to be modeled. A typical f_d, 0° flap and $u_0 = 57m/sec$, with the system sampled at 100Hz is

$$f_d = \begin{bmatrix} -0.0039 \\ -0.0152 \\ 0.0000 \\ 0.0015 \end{bmatrix}. \tag{8}$$

Detection Space

The first part in the design of a BJDF is to determine the detection space of the event vector. This is important as the detection space contains all the failure event vectors that are equivalent. Additionally the rank of the detection space indicates the number of poles of the estimator which are determined by the geometric constraints of the detection filter. Jones, [4], defines the detection space of f_d, $\overline{\mathcal{R}}_1$, in the following manner.

Definition 1. Let f_d be an event vector associated with a failure in a system which is modeled in the un-failed state by (A, B, C). Let $Cf_d \neq 0$. The detection space for f_d is denoted by $\overline{\mathcal{R}}_1$ and is the direct sum:

$$\overline{\mathcal{R}}_1 = f_d \oplus \mathcal{R}_1 \tag{9}$$

where $\mathcal{R}_1$ is the largest subspace which satisfies the three conditions:

$$\mathcal{N}(\mathcal{O}) \cap \mathcal{R}_1 = \emptyset \tag{10}$$

$$\mathcal{R}_1 \subset \mathcal{N}(C) \tag{11}$$

$$A\mathcal{R}_1 \subset \overline{\mathcal{R}}_1 \tag{12}$$

where $\mathcal{O}$ is the system observability matrix.

The procedure to determine the detection space of f_1 is straight forward and documented in [3] and [4]. Use the failure signature to define a decoupling feedback gain, D_f, and a new output matrix C_m,

$$D_f = Af_d((Cf_d)^T(Cf_d))^{-1}(Cf_d)^T \tag{13}$$

$$C_m = (I - Cf_d((Cf_d)^T Cf_d)^{-1}(Cf_d)^T)C \tag{14}$$

then form the system observability matrix, $\mathcal{O}$ for this system.

$$\mathcal{O} = \begin{bmatrix} C_m \\ C_m(A - D_f C) \\ \vdots \\ C_m(A - D_f C)^{n-1} \end{bmatrix}. \tag{15}$$

The detection space is then just the null space of this matrix, $\mathcal{O}$. Let $g = \overline{\mathcal{R}}_1$ and for the example case (8) the detection space, g, is

$$g = \begin{bmatrix} -0.2457 \\ -0.9647 \\ 0.0005 \\ 0.0947 \end{bmatrix}, \tag{16}$$

and when passed through the output matrix C this results in the residual projection vector

$$g_c = Cg = \begin{bmatrix} -0.1716 \\ 0.0048 \\ 0.9852 \end{bmatrix}, \tag{17}$$

BJDF Design for Flight Test Data

The design of the BJDF for the flight test data has four degrees of freedom. The closed loop poles must be selected. The first closed pole is the pole associated with the detection vector space. In this case the pole was placed at $\lambda = 0.97$. This roughly corresponds to the linearized short period dynamics, $w_{sp} = 3rad/sec$, sampled at 100Hz and was found to give good results. Further research needs to be done to determine the optimal choice for this pole location. The choice of this pole determines part of the total feedback gain, $D_g = D_{P1} + D_{P2}$, where

$$D_{P1} = (-\lambda f_d + A f_d)((Cf_d)^T(Cf_d))^{-1}(Cf_d)^T. \quad (18)$$

The system can then be decomposed in the unobservable part caused by this feedback gain and the still available observable part. The poles of the remaining observable part, P =closed loop poles, were placed by using Linear Quadratic Estimator theory and for the example used above were placed at

$$P = \begin{bmatrix} 0.38 \\ 0.99 \\ 0.97 \end{bmatrix}. \quad (19)$$

The simulated performance of the gain scheduled detection filter is shown in Figure 1, Figure 2, and Figure 3. Figure 1 shows the directional error, $e_{dir} = g_c^T e$, versus time for the simulated noiseless nominal and iced cases. The constant difference between the nominal case and the iced case from the start of the simulation to the start of the elevator input is the error due to the trim change because of icing. The larger errors occur when the elevator excitation occurs and represent the reduction in the input matrix, B. In Figure 2 and Figure 3 the magnitude of $e_{dir} = g_c^T e$ is plotted versus the angle between the two vectors. This is the magnitude of the error in the failure detection space.

Results

The nominal flight test cases and the failed boot flight test cases were run throught the gain scheduled BJDF. The results are presented in Tables 1 through 5, where α_0 is the trim angle of attack and U_0 is the airspeed in meters/sec.. In all but one case, high α and $\delta_{Flap} = 0$, the maximum directional error for the failed boot case was higher than the nominal case. The one case where this is not true is not a

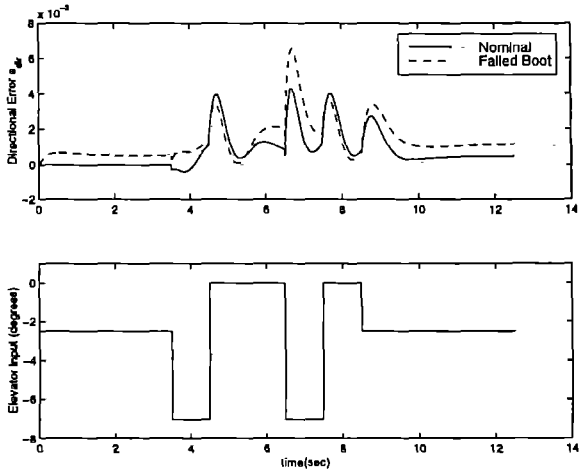

Figure 1: Simulated Directional Error and Elevator Input $\delta_{flap} = 0°, \alpha_0 \approx 3.5°, u_0 \approx 57m/sec$

practical flight condition for commercial twin turboprop aircraft. In Figure 4 the directional error and elevator input are shown for two comparable iced and nominal cases. Although there is not enough data to drawn any statistical conclusions the ratio of failure signal to nominal signal in Table 1 is ≈3.2. In Figures 5 and 6 $|e_{dir}|$ is plotted versus the angle bewtween g_c and e. In Figure 4 the two large error spikes at 6 and 8 seconds in Figure 4 can be seen as the two large excursions from the ball near zero in Figures 5 and 6. These spikes correspond to the periods of greatest excitation.

In Figure 7 the case of $\delta_{Flap} = 30°$ is shown. The polar plots of the errors are shown in Figures 9 and 8. The ratio of the failure signal to the nominal signal in Table 4 is as high as ≈3. This indicates that at this flap setting there is a very good chance that icing can be detected. This is also the most dangerous circumstance since it is near tail stall. When the flight test were being performed the elevator authority went virtually to zero at $\delta_{Flap} = 40°$. At high α and high δ_{Flap} a plane undergoing icing has a low tail stall margin. This has been known but it is also clear from the amount of error produced by the detection filter under such conditions.

Further work needs to be done to determine the best signal processing to be done on the error residuals to minimize detection errors. Additionally the optimal pole placement of the detection filter poles needs to be investigated.

Conclusion

Preliminary results of a technique for detecting air-

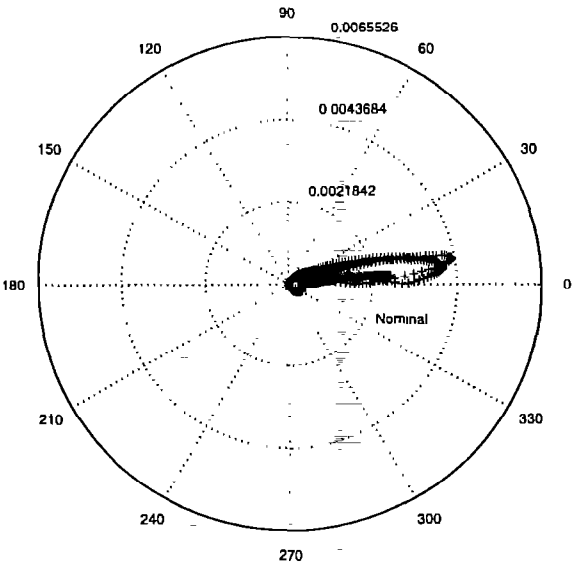

Figure 2: Simulated Directional Error Polar Plot $\delta_{flap} = 0°, \alpha_0 \approx 3.5°, u_0 \approx 57m/sec$

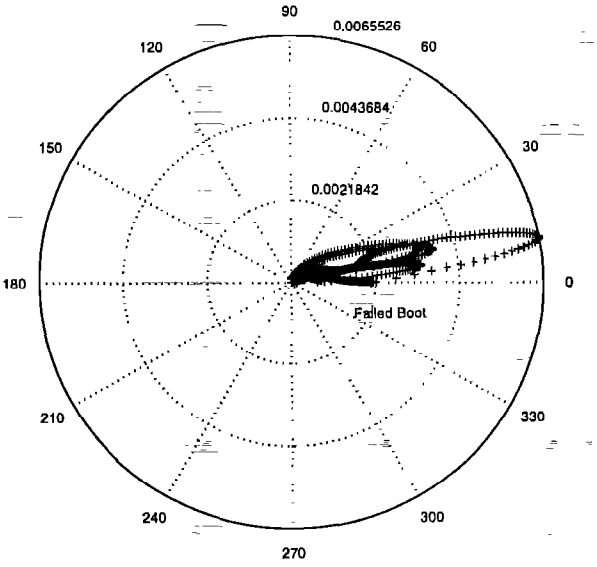

Figure 3: Simulated Directional Error Polar Plot $\delta_{flap} = 0°, \alpha_0 \approx 3.5°, u_0 \approx 57m/sec$

Table 1 $\delta_{Flap} = 0°$			
Failed Boot	α_0	U_0	Directional e_{max}
F	3.57	56.7	0.0126
N	3.50	58.1	0.0040
F	5.45	51.6	0.0070
N	4.76	52.2	0.0042
F	7.53	46.9	0.0069
N	7.02	46.9	0.0043
F	11.01	41.3	0.0027
N	10.68	41.3	0.0029

Table 2 $\delta_{Flap} = 10°$			
Failed Boot	α_0	U_0	Directional e_{max}
F	-1.46	57.8	0.1218
N	-1.61	56.6	0.1039
F	-0.14	52.7	0.0981
N	-0.19	50.9	0.0967
F	1.77	46.1	0.0850
N	1.82	44.9	0.0511
F	4.32	41.2	0.0699
N	4.47	40.0	0.0491

craft icing by continuously estimating control surface effectiveness have been presented. A BJDF was used which is not concerned with attempting to measure the ice accretion but rather with the deleterious effects on aircraft controllability. Finally the BJDF method was applied to icing research flight test data from NASA Lewis and the viability of the method demonstrated.

Acknowledgments

The authors would like to thank Thomas Ratvasky of NASA Lewis Research Center and Judith Van Zante of NYMA for their helpful discussions and comments. The flight test data was generously supplied by NASA Lewis Research Center. Also Dr. Gene Morelli of NASA Langley provided assistance with the SWR, stepwise regression, flight test data fitting code from NASA Langley.

References

[1] P.M. Render, L.R. Jenkinson. Investigation into Ice Detection Parameters for Turboprop Aircraft. *Journal of Aircraft*, 33(1):125–129, January-February 1996.

[2] IFAC World Congress. *Parameter Identification for inflight Detection of Aircraft Iciing*, July 1999.

[3] Richard Beard. *Failure Accomodation in Linear Systems through Self-Reorganization.* PhD thesis, MIT, 1971.

[4] Harold Jones. *Failure Detection in Linear Systems.* PhD thesis, MIT, 1973.

[5] Robert H. Miller and William B. Ribbens. The Effects of Icing on the Longitudinal Dynamics of

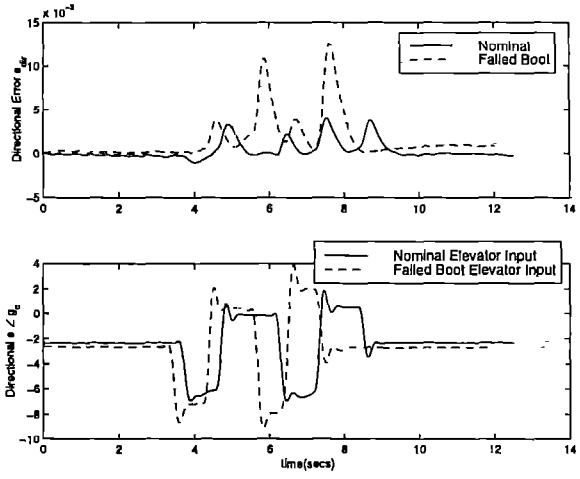

Figure 4: Directional Error and Elevator Input $\delta_{flap} = 0°, \alpha_0 \approx 3.5°, u_0 \approx 57m/sec$

Table 3 $\delta_{Flap} = 20°$			
Failed Boot	α_0	U_0	Directional e_{max}
F	-2.92	49.1	0.0381
N	-2.97	47.1	0.0311
F	-1.11	43.9	0.0385
N	-0.97	42.4	0.0237
F	2.38	36.8	0.0237
N	1.58	37.5	0.0171
F	6.95	32.2	0.0169
N	6.33	32.6	0.0144

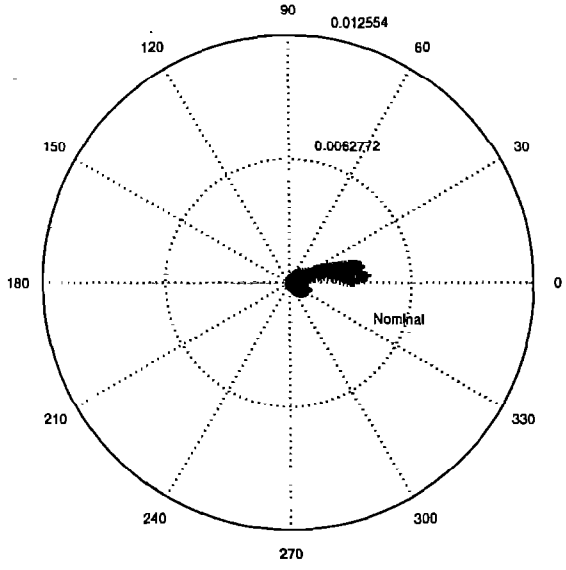

Figure 5: Nominal Directional Error Polar Plot $\delta_{flap} = 0°, \alpha_0 \approx 3.5°, u_0 \approx 57m/sec$

an Icing Research Aircraft. Number 99-0636 in 37th Aerospace Sciences. AIAA, Jan. 1999.

[6] Thomas P. Ratvasky and Judith Foss Van Zante. NASA/FAA Tailplane Icing Program Overview. Number 99-370 in 37th Aerospace Sciences. AIAA, Jan. 1999.

[7] Thomas P. Ratvasky and Judith Foss Van Zante. In-Flight Aerodynamic Measurements of an Iced Horizontal Tailplane. Number 99-0638 in 37th Aerospace Sciences. AIAA, Jan. 1999.

[8] Judith Foss Van Zante and Thomas P. Ratvasky. Investigation of Dynamic Flight Maneuvers with an Iced Tailplane. Number 99-0371 in 37th Aerospace Sciences. AIAA, Jan. 1999.

[9] John H. Blakelock. *Automatic Control of Aircraft and Missles.* John Wiley, 2nd edition edition, 1991.

Table 4 $\delta_{Flap} = 30°$			
Failed Boot	α_0	U_0	Directional e_{max}
F	-5.04	46.2	0.0716
N	-5.65	47.1	0.0561
F	-3.33	42.2	0.0771
N	-4.12	42.5	0.0258
F	-0.59	37.1	0.0605
N	-0.98	35.5	0.0230
F	4.11	31.7	0.0470
N	3.09	31.5	0.0146

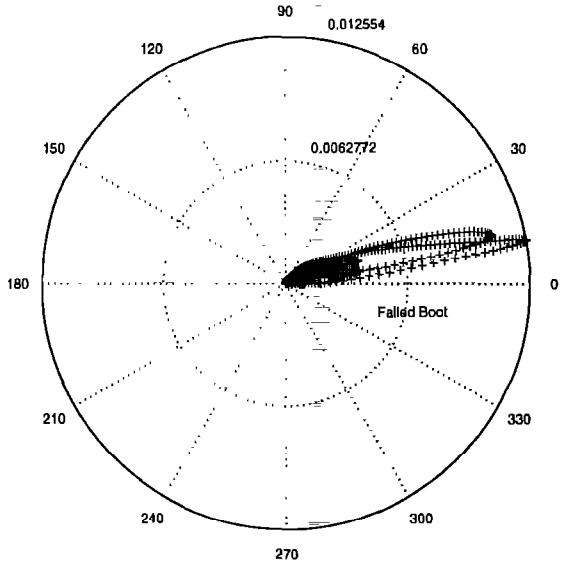

Figure 6: Failed Boot Directional Error Polar Plot $\delta_{flap} = 0°, \alpha_0 \approx 3.5°, u_0 \approx 57m/sec$

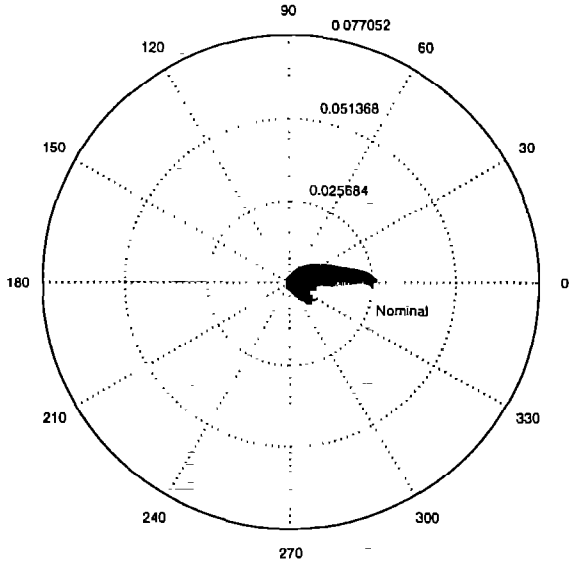

Figure 8: Directional Error Polar Plot $\delta_{flap} = 30°, \alpha_0 \approx -3.5°, u_0 \approx 42.4m/sec$

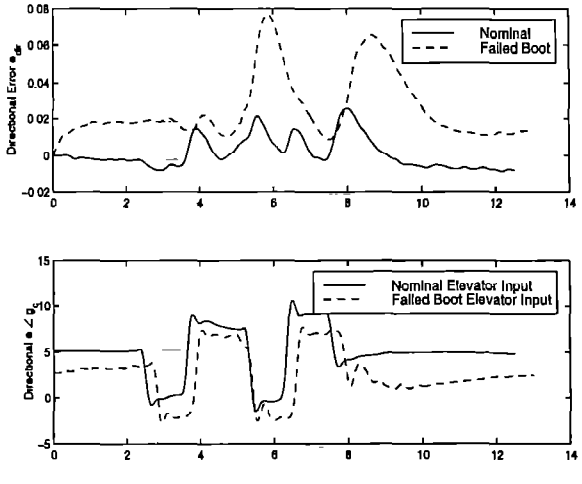

Figure 7: Directional Error and Elevator Input $\delta_{flap} = 30°, \alpha_0 \approx -3.5°, u_0 \approx 42.4m/sec$

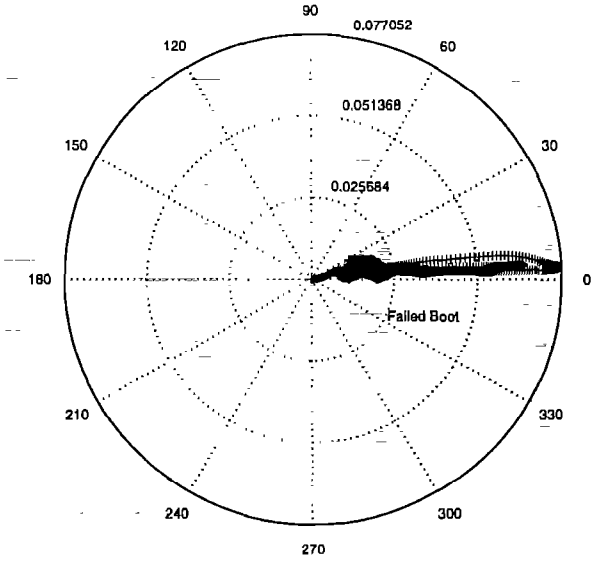

Figure 9: Directional Error Polar Plot $\delta_{flap} = 30°, \alpha_0 \approx -3.5°, u_0 \approx 42.4m/sec$